Chinese Chemical Letters 32 (2021) 102–106

Contents lists available at ScienceDirect

Chinese Chemical Letters

journal homepage: www.elsevier.com/locate/cclet

Communcation

A novel polyethyleneimine-decorated FeOOH nanoparticle for efficient siRNA delivery

Shuai Guo[a], Bei Liu[b], Mengjie Zhang[a], Chunhui Li[a], Xiaoxia Wang[f], Yuhua Weng[a,e], Lele Li[b,d], Yuanyu Huang[a,c,*]

[a] School of Life Science, Advanced Research Institute of Multidisciplinary Science, Key Laboratory of Molecular Medicine and Biotherapy, Institute of Engineering Medicine, Beijing Institute of Technology, Beijing 100081, China
[b] CAS Key Laboratory for Biomedical Effects of Nanomaterials and Nanosafety, CAS Center for Excellence in Nanoscience, National Center for Nanoscience and Technology (NCNST), Beijing 100190, China
[c] School of Pharmacy, Hunan University of Chinese Medicine, Changsha 410208, China
[d] College of Materials Science and Optoelectronic Technology, University of Chinese Academy of Sciences, Beijing 100049, China
[e] Hunan University of Science and Engineering, Yongzhou 425199, China
[f] Institute of Molecular Medicine, Peking University, Beijing 100871, China

ARTICLE INFO

Article history:
Received 21 August 2020
Received in revised form 9 November 2020
Accepted 11 November 2020
Available online 20 November 2020

Keywords:
FeOOH
siRNA delivery
RRM2
RNA interference
Polyetherimide
Cancer treatment

ABSTRACT

Despite the promising prospect of small interfering RNA (siRNA) for the treatment of diverse diseases, it remains challenging to develop novel delivery materials to desired tissues and cells. In this study, a novel iron oxyhydroxide (FeOOH) nanoparticle (NP) whose surface was modified with branched polyetherimide (PEI) was developed to deliver siRNA into the cancer cells. It was demonstrated that PEI-FeOOH (PFeOOH) efficiently complexed siRNA, mediated effective cellular uptake and endosomal escape, thereby triggering robust gene silencing *in vitro*. In addition, PFeOOH/siRNA formulation loading with anti-RRM2 siRNA effectively inhibited the growth of tumor tissues, and exhibited excellent safety profiles *in vivo*. Therefore, this study conceptually provided a FeOOH-based nucleic acid delivery vesicle which can potentially use to achieve diagnosis and therapy simultaneously.

ONPATTRO® (patisiran) and GIVLAARI® (givosiran) are two small interfering RNA (siRNA) therapeutics that were approved by the U.S. Food and Drug Administration (FDA) in 2018 and 2019, respectively [1–3]. These events have greatly promoted the development of nucleic acid therapeutics and raised the field to a new stage. In theory, siRNA can target any gene and down-regulate its expression, therefore siRNA-based therapeutics are under development for the treatment of various diseases including viral infections [4,5], hereditary disorders [6,7] and cancers [8–10]. Despite of great success of *N*-acetylgalactosamine (GalNAc)-siRNA conjugate delivery platform for liver-targeted oligonucleotide delivery, it remains challenging to develop efficient delivery materials to other desired tissues and cells, especially for the cancer cells [11–17].

Inorganic materials constitute a kind of important and effective delivery vesicles, which have been investigated for nucleic acid delivery for decades [18–24]. The major advantages of inorganic materials include: controllable particle sizes, large surface areas, low toxicity, ease of surface functionalization, good biocompatibility and ability to protect the housed drugs from degeneration or denaturation, *etc*. [25–28]. In the field of inorganic nanomaterials, the carriers used for biomedical application can basically be categorized into two classes. One takes advantage of structural characteristics involving void morphology, such as porosity or hollow interiors, which can be used to serve as nanocon-tainers, acting as capsulelike carriers and provide protection to limit the accessibility of the biomolecules and drugs to denaturing agents [29–31]. Meanwhile, for inorganic nanomaterials like nanoparticles (NPs) and nanorods, attaching desirable biomolecular signals or drugs on their surface is another appropriate delivery method. [32,33]. However, the preparation of the first kind of nanocomposites is complicated and usually takes several days, which are unsuitable for scaled-up production. To overcome those hurdles, a facile synthetic method is needed as an inorganic nanoplatform for drug delivery.

* Corresponding author at: School of Life Science, Advanced Research Institute of Multidisciplinary Science, Key Laboratory of Molecular Medicine and Biotherapy, Institute of Engineering Medicine, Beijing Institute of Technology, Beijing 100081, China.
E-mail addresses: yyhuang@bit.edu.cn, yyhuang@pku.edu.cn (Y. Huang).

https://doi.org/10.1016/j.cclet.2020.11.024
1001-8417/

Iron oxyhydroxide (FeOOH) is an aqueous iron oxide mineral with feature of stable chemical properties, relatively large specific surface areas, excellent particle structures and advantages of being cheap, easy to obtain and better decomposition, and it has a certain adsorption capacity for organic matter [34,35]. In addition, iron oxyhydroxide is a precursor used for synthesis of magnetic materials magnetite, maghemite and hematite in the industrial application [36]. In the low pH range, the proton H^+ in the Iron oxide solution has a strong affinity with O^{2-} of the structure, and Fe^{3+} in the iron mineral is released into the solution. Moreover, it may become a T1 magnetic resonance contrast agent with acid responsive property [30].

Currently, FeOOH-based NPs have mainly been used in photocatalytic reaction [37,38] and waste water treatment [39], while the examples of the development and application of polyelectrolyte FeOOH as biomolecular carriers is barely reported. Herein, we presented a protocol for synthesizing FeOOH NPs whose surface were modified with branched polyetherimide (PEI), with molecular weight of 25 kD, which were then employed to condense siRNA, forming siRNA-loaded PEI-FeOOH (PFeOOH/siRNA) complexes that enable siRNA transfection into cancer cells (Scheme 1). To our knowledge, this is the first example using polymer-decorated FeOOH NPs to deliver siRNA *in vitro* and *in vivo*. Considering its imaging potential [40,41], this work established a possibility that FeOOH-based NPs can be used to deliver genes or drugs, and to achieve diagnosis and treatment simultaneously.

In this study, the spindle-shaped (β-FeOOH) NPs were prepared by forced hydrolysis of diluted aqueous iron chloride ($FeCl_3{\cdot}6H_2O$) solution [39,42]. During hydrolysis, the colour of the aqueous iron chloride solution slowly changed from light yellow to deep brown, indicating the formation of β-FeOOH NPs. Then, the positively-charged and branched PEI was modified on the FeOOH particles surface to form PEI-coated FeOOH NPs. The product, PFeOOH NPs, with the highest quality in homogeneity and dispersion were successfully prepared. It was revealed that 5 mL of the prepared PFeOOH ethanol solution was dried and weighed to 6 mg. Fig. 1A shows a typical TEM image of the as-synthesized PFeOOH products with lengths of approximate 90 nm.

The capability of PFeOOH NPs in binding siRNA was evaluated with gel retardation assay (Fig. 1B). PFeOOH ethanol solution (1 mL) was mixed with 1.2 mL of ddH_2O to prepare a PFeOOH solution with a mass concentration of 1 mg/mL. Then it was mixed with siRNA solution (0.2 mg/mL) at the volume ratios of 1:1, 3:1, 5:1, 7:1, 9:1 and 15:1, whose mass ratios were 5:1, 15:1, 25:1, 35:1, 45:1, 75:1, respectively. Electrophoresis data showed that siRNA can be well entrapped by electrostatically interacting with the PFeOOH NPs when the volume ratio was higher than 3:1 (mass ratio was higher than 15:1). However, it is usually necessary to use a ratio higher than the cut-off value (3:1), because if the ratio is close to 3:1, the siRNA may depolymerize from the nanoparticles if using them under complicated environment.

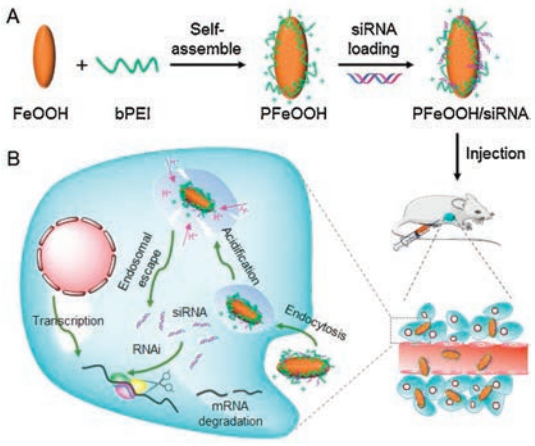

Scheme 1. Schematic illustration of siRNA delivery mediated by PFeOOH NPs. (A) Formation of PFeOOH NPs and PFeOOH/siRNA complexes. (B) Cartoon illustration of the PFeOOH/siRNA complexes for targeted siRNA delivery and RNA interference (RNAi) pathway.

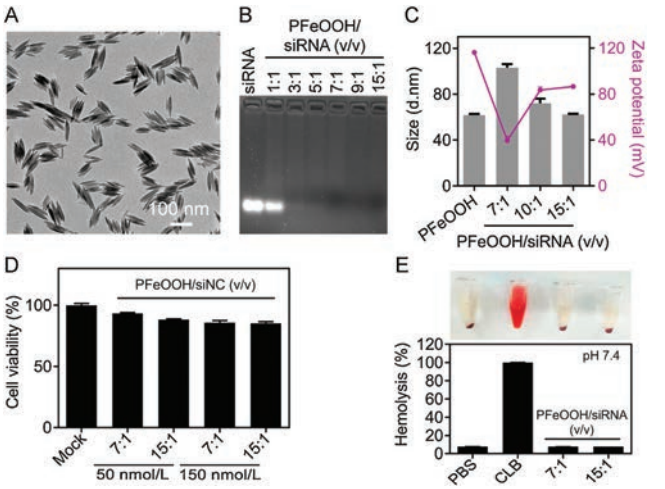

Fig. 1. Characterization of PFeOOH NPs. (A) TEM image of PFeOOH NPs. (B) Gel retardation analysis of PFeOOH/siRNA complexes. (C) Particle sizes and zeta potentials of functionalized PFeOOH/siRNA complexes ($n = 3$). (D) Cytotoxicity was measured using MTT assay ($n = 6$). (E) Serum stability assays by hemolysis experiment. CLB, cell lysis buffer ($n = 3$). Data in (B), (D) and (E) were shown as the mean ± SEM.

To further characterize the interaction between PFeOOH and siRNA, the size distribution and zeta potential of siRNA-loaded PFeOOH NPs at various volume ratios were measured (Fig. 1C). Compared to empty vehicles (PFeOOH) (62 nm), the sizes of PFeOOH/siRNA complexes were relatively larger than the empty vehicles when the the volume ratio of PFeOOH and siRNA was 7:1, which showed an average diameter of 103 nm. But interestingly, with volume ratios further increased, the sizes gradually decreased, even reached 62 nm again at volume ratio of 15:1 (v_{PFeOOH}: v_{siRNA}) (Fig. 1C). The zeta potential of empty NPs was 116 mV. With the increase of volume ratio from 7:1 to 10:1 and 15:1, the zeta potentials of PFeOOH/siRNA complexes increased from 39 mV to 84 mV and 87 mV, respectively (Fig. 1C). Due to the electrostatic repulsion between the nanoparticles, the positive surface charge helps prevent the nanoparticles from aggregating. Altogether, PFeOOH/siRNA formulations with volume ratios of 7:1 and 15:1 (mass ratios of 35:1 and 75:1) were selected and used for the following experiments.

In vitro MTT assay and hemolysis test were performed to evaluate the biocompatibility of the complexes. Firstly, PFeOOH/siRNA with volume ratios of 7:1 and 15:1 were assessed at the transfection concentrations of 50 nmol/L and 150 nmol/L respectively, which proved that these formulations have ideal biocompatibility (Fig. 1D). Then cytotoxicity was further evaluated by testing PFeOOH/siRNA nanoparticles with higher volume ratios (20:1, 30:1, 40:1, 50:1, 80:1 and 100:1, the transfection concentration was 50 nmol/L) and at higher transfection concentrations (300 nmol/L and 600 nmol/L, v/v = 15:1). Data showed that no obvious cytotoxicity was observed for all tested formulations (Fig. S1 in Supporting information). In addition, red blood cells (RBCs) samples were treated with PBS buffer, cell lysis buffer (CLB), and PFeOOH/siRNA formulations at volume ratios of 7:1 and 15:1 at pH 7.4 for 2 h at 37 °C, respectively. Consistent with the results of MTT, no hemolysis was observed for the samples treated with PBS

and PFeOOH/siRNA formulations, while significant hemolysis was displayed for CLB-treated sample (Fig. 1E). Therefore, it was preliminarily proved that PFeOOH vehicles have good biocompatibility and can be used for animal experiments.

To determine the suitability of PEI-FeOOH NPs as MRI contrast agent, the MRI performances of PEI-FeOOH NPs were studied using MR scanner. With the increase in the PEI-FeOOH NPs concentration, the T2-weighted MRI signal increased gradually (negative contrast effect) (Fig. S2 in Supporting information), indicating the promising potential of PEI-FeOOH NPs in the MR imaging of tumors.

To investigate the cellular uptake and subcellular localization of different complexes *in vitro*, 4T1 cells, a murine mammary carcinoma cell line from a BALB/cfC3H mouse, were treated with free Cy5-labelled siRNA (Cy5-siRNA) (50 nmol/L), lipofectamine 2000(Lipo)/Cy5-siRNA (50 nmol/L), PFeOOH/Cy5-siRNA (50 nmol/L and 150 nmol/L) at volume ratios of 7:1 and 15:1 for 4 h. Subsequently, cell were analysed with confocal laser scanning microscopy (CLSM) or fluorescence-activated cell sorting (FACS).

As shown in Fig. 2A, the Cy5 signal of the all PFeOOH/Cy5-siRNA groups could be clearly observed in the cells, and the signal intensities were comparable to that of Lipo/Cy5-siRNA. Most of red fluorescence signals (Cy5-siRNA) did not co-localize with the green fluorescence signal (endosome and lysosome that stained with lysotracker green). In contrast, almost no Cy5 signal was observed in naked Cy5-siRNA group. These data indicated that the PFeOOH NPs mediated effective siRNA transfection into the cancer cells *in vitro*. Due to the rapid proton adsorption of PEI in acidic environment of the endosome, the pH in the organelles increased and proton sponge effects were induced. Finally, endosomes were swollen and ruptured, and the siRNAs were released into the cytoplasm.

In addition, the intracellular fluorescence intensity and cell percentages with internalized Cy5-labeled siRNA were evaluated *via* flow cytometry (Figs. 2B and C). Compared to the untreated cells, when the final siRNA concentration was 50 nmol/L, the averaged percentages of Cy5-siRNA positive cells were 79% and 75% at volume ratios of 7:1 and 15:1, respectively. When the final siRNA concentration was 150 nmol/L, the percentages at volume ratios of 7:1 and 15:1 were 91% and 89%, respectively. These data indicated that endocytosis rate of cells transfected with 150 nmol/L of PFeOOH/Cy5-siRNA was slightly higher than that of cells treated with 50 nmol/L of PFeOOH/Cy5-siRNA. These results were in line with the confocal observations showed in Fig. 2A. In addition, when the transfection concentration was the same, no significant difference was observed between the cells treated with PFeOOH/Cy5-siRNA at volume ratios of 7:1 and 15:1.

To explore gene silencing efficiencies of several complexes with different volume ratios *in vitro*, we measured RRM2 mRNA expression in 4T1 cells after 24 h transfection by real-time

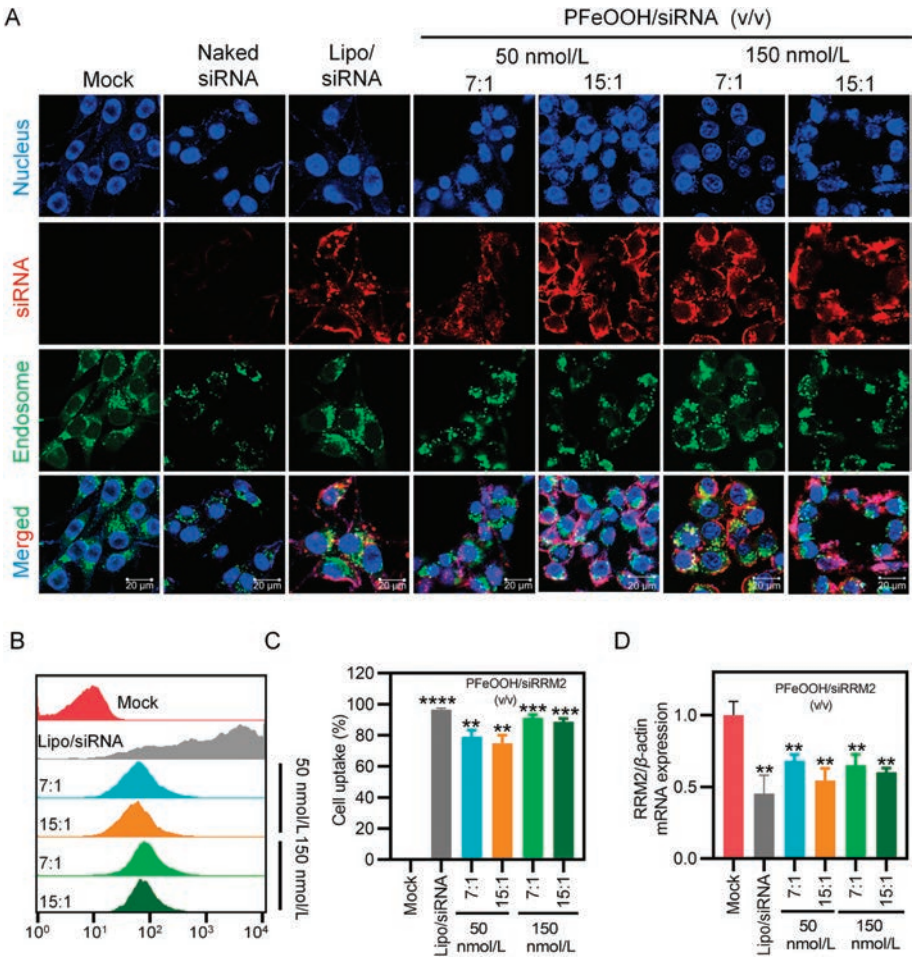

Fig. 2. *In vitro* subcellular localization, cellular uptake, and gene silencing of PFeOOH/siRNA complexes in 4T1 cells. (A) Intracellular localization was observed by CLSM. Blue, nuclei stained by Hoechst 33342; green, endosomes and lysosomes stained by LysoTracker green; red, Cy5-siRNA. Scale bar is 20 μm. (B, C) Cellular uptake of Cy5-siRNA detected by flow cytometry (B) and quantitative analysis of Cy5-labelled positive cell rates (C). (D) RRM2 mRNA expression of 4T1 cells after being treated with PFeOOH/siRNA complexes at the final siRNA concentrations of 50 nmol/L and 150 nmol/L. Each bar represents mean ± SEM of three experiments. Statistical analysis was performed with two-tailed student *t*-test. $^{**}P < 0.01$; $^{***}P < 0.001$ *vs.* the Mock group.

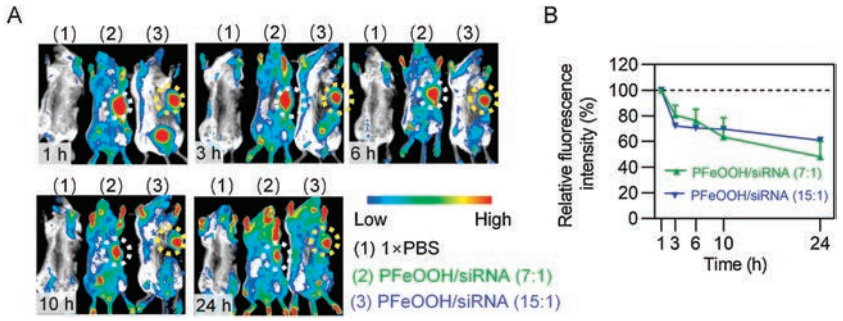

Fig. 3. *In vivo* fluorescence imaging and quantitative analysis of the 4T1 xenograft tumor-bearing BABL/c mice following i.t. injection of PBS, PFeOOH/siRNA (7:1) and PFeOOH/siRNA (15:1). (A) Whole-body imaging of representative mice acquired at the indicated time points post injection. (B) Relative fluorescence intensities in the tumor regions determined by normalizing to the initial fluorescence intensity of each group ($n = 3$). Data were shown as the mean ± SEM.

quantitative PCR (RT-qPCR) (Fig. 2D). As reported, RRM2 catalyzes the formation of deoxyribonucleotides and is essential for DNA synthesis. Inhibition of RRM2 activity in proliferating cancer cells rapidly induces mitotic arrest and apoptosis, which makes it an ideal cancer therapeutic gene [43,44]. As shown in Fig. 2D, compared to the mock group, all four treatments with PFeOOH/Cy5-siRRM2 complexes remarkably inhibited RRM2 mRNA expression with approximate 40% inhibition efficiency at 50 nmol/L transfection concentration and around 50% repression efficiency at 150 nmol/L transfection concentration, respectively. Lipo2000/siRNA, the positive control, showed slightly higher internalization and gene silencing efficiencies than PFeOOH/siRNA nanoparticles. Altogether, it was demonstrated that PFeOOH NP is an effective delivery material capable of delivering siRNA to cancer cells and mediating robust down-regulation of gene expression *in vitro*.

Drug retention and metabolism in the tumors are crucial for effective cancer treatment. Therefore, we further evaluated the accumulation and elimination of PFeOOH/siRNA complexes within 24 h after injection. Mice displaying tumor volumes around 400 mm^3 were randomly divided into three groups and received the treatments of PBS, PFeOOH/Cy5-siRNA (7:1) and PFeOOH/Cy5-siRNA (15:1) by intratumoral (i.t.) injection. Whole-body fluorescence images of the mice were acquired over 24 h, and the signals of tumor sites were quantitatively analysed (Figs. 3A and B). The fluorescence signals of tumor sites for PFeOOH/ Cy5-siRNA (7:1) and PFeOOH/Cy5-siRNA (15:1) groups were strong and comparable within 24 h. They firstly declined at 3 h post injection, and then slowly decreased within 24 h post injection. The elimination rate of PFeOOH/Cy5-siRNA (7:1) complexes was close to that of PFeOOH/Cy5-siRNA (15:1) complexes in the tumors. Together with the data shown in Figs. 1 and 2, we chose PFeOOH/Cy5-siRNA NPs (7:1) for the following anticancer experiments.

Motivated by the decent biocompatibility, effectiveness *in vitro* and retention in tumor of PFeOOH/siRNA, the anticancer effect of proposed formulation was further evaluated in 4T1 xenograft tumor-bearing BABL/c mice. When the tumor volumes grew to approximately 450 mm^3, they were randomly divided into three groups and treated with PBS, PFeOOH/siNC and PFeOOH/siRRM2 by i.t. injection every other day for 9 consecutive days. Tumor growth and body weight were recorded for 9 days. The tumor volumes were normalized to the volumes recorded at the starting points, which represented the relative fold changes of tumors during the treatment course. As shown in Fig. 4A, the mice treated with PFeOOH/siNC NPs did not exhibit tumor suppression

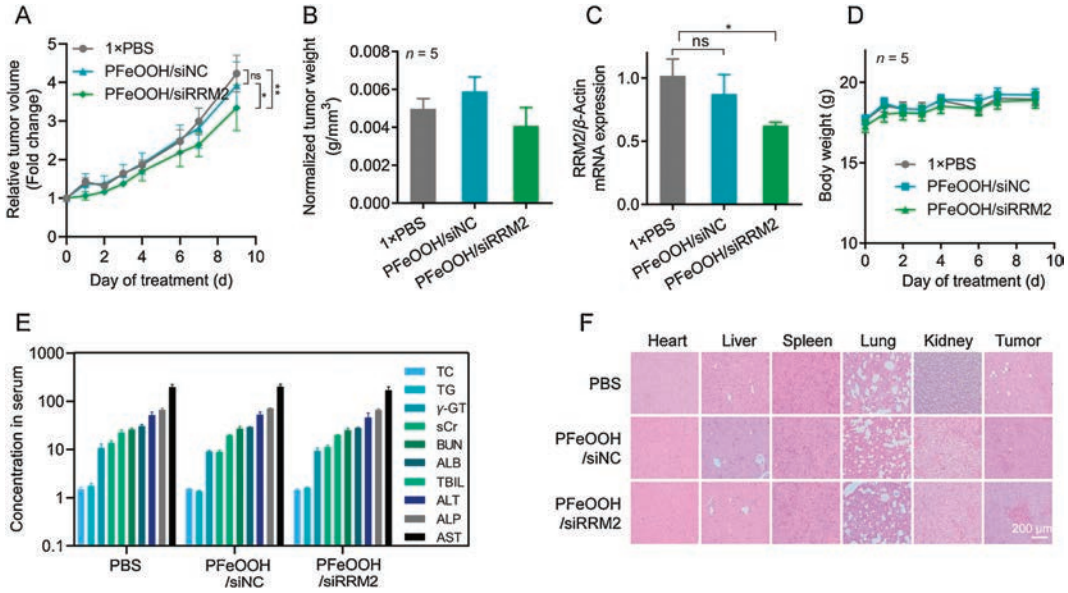

Fig. 4. Antitumor effect of siRRM2-loaded PFeOOH NPs in 4T1 tumor-bearing BABL/c mice. (A) Relative fold changes of tumor volumes normalized to the starting point. (B) Normalized average tumor weights at the end observation time. The tumor weights of the animals were normalized to the corresponding tumor volumes of the animals recoded at the starting point, which could erase the influence of differences of tumor sizes on the final treatment efficacy. (C) Expression of RRM2 mRNA in tumor tissues. (D) Changes in body weight of the animals. (E) Serum biochemistry parameters measured in mouse specimens collected at the end time point. (F) Histological assessments of major organs and tumor tissues using H&E staining. Data are presented as mean ± SEM. $^*P < 0.05$; $^{**}P < 0.01$; ns, no significant difference was observed. $n = 5$.

compared to the PBS group. While PFeOOH/siRRM2 exhibited acceptable inhibitory effect compared to the PBS group and the PFeOOH/siNC group (Fig. 4A). Although tumors in PFeOOH/siRRM2 group still grew during the treatment course, which may be attributed to the tumors were too large ($\sim$ 450 mm^3) when we started to treat, significantly difference was observed between PFeOOH/siRRM2 and PFeOOH/siNC, and between PFeOOH/siRRM2 and PBS. At the end time point, the mice were uniformly sacrificed and dissected, and the tumors were weighed. The normalized tumor weight revealed consistent pattern (Fig. 4B). The expressions of RRM2 in tumor tissues were significantly repressed in the mice receiving the treatment of PFeOOH/siRRM2 nanoparticles (Fig. 4C). Moreover, the body weights of all groups increased during the treatment course (Fig. 4D). To further assess the toxicity *in vivo*, blood of mice was obtained for serum biochemical analysis. Tumors and different organs, including the heart, the liver, the spleen, the lungs, and the kidneys were collected, fixed, embedded, and stained for histopathological observation. As shown in Fig. 4E, there was no obvious change of markers of liver or kidney function in serum for these three groups. No distinct pathological change was observed in the major organs of PBS, PFeOOH/siNC and PFeOOH/siRRM2 groups, and apoptosis was observed in tumor received PFeOOH/siRRM2 treatment, as the arrowhead indicated (Fig. 4F).

In summary, we here designed and constructed PEI-coated FeOOH NPs as a vehicle to deliver siRNA *in vitro* and *in vivo*. Flow cytometry and confocal microscopy data proved that the PFeOOH/siRNA NPs were able to be swallowed by 4T1 cells and escape from endosomes/lysosome, which triggered robust gene silencing *in vitro*. No significant cytotoxicity was observed in MTT and hemolysis assays. In addition, the functionalized siRRM2-loaded PFeOOH NPs exhibited ideal drug retention in tumor tissues, effective anticancer effects, and an excellent safety profile *in vivo*. Therefore, we believe the PFeOOH NPs is a promising carrier in siRNA or drugs delivery for therapeutic development. In addition, the amine groups on the shells (the PEI polymer) of the NPs actually can provide further surface modification for attachment of other functional groups, such as targeting moieties or imaging reagent, which may expand the applications of proposed nanostructures.

Declaration of competing interest

The authors report no declarations of interest.

Acknowledgments

This work was supported by the Hunan Provincial Natural Science Foundation of China (Nos. 2018JJ1019, 2019JJ50196), the Hu-Xiang Young Talent Program (No. 2018RS3094), the National Natural Science Foundation of China (Nos. 31871003, 31901053), the Beijing Institute of Technology Research Fund Program for Young Scholars and the Fundamental Research Funds for the Central Universities (No. 2018CX01023), the Beijing-Tianjin-Hebei Basic Research Cooperation Project (No. 19JCZDJC64100), the Beijing Nova Program from Beijing Municipal Science & Technology Commission (No. Z201100006820005), the Young Elite Scientist Sponsorship Program of Beijing Association for Science and Technology (2020-2022). We thank Biological & Medical Engineering Core Facilities (Beijing Institute of Technology) for providing advanced equipment and help.

Appendix A. Supplementary data

Supplementary material related to this article can be found, in the online version, at doi:https://doi.org/10.1016/j.cclet.2020.11.024.

References

[1] Y. Weng, H. Xiao, J. Zhang, et al., Biotechnol. Adv. 37 (2019) 801–825.
[2] Y.Y. Huang, Prog. Biochem. Biophys. 46 (2019) 313–322.
[3] B. Hu, Y. Weng, X.H. Xia, et al., J. Gene Med. 21 (2019) e3097.
[4] J. Beloor, N. Maes, I. Ullah, et al., Cell Host Microbe 23 (2018) 549–556.
[5] Y. Yang, T. Liu, D. Shen, et al., PLoS Pathog. 15 (2019) e1007534.
[6] M. Jimenez-Sanchez, W. Lam, M. Hannus, et al., Nat. Chem. Biol. 11 (2015) 347–354.
[7] P.J. Schmidt, I. Toudjarska, A.K. Sendamarai, et al., Blood 121 (2013) 1200–1208.
[8] V. Veschi, Z. Liu, T.C. Voss, et al., Cancer Cell 31 (2017) 50–63.
[9] S. Wang, X. Liu, S. Chen, et al., ACS Nano 13 (2019) 274–283.
[10] C. Xu, D. Li, Z. Cao, et al., Nano Lett. 19 (2019) 2688–2693.
[11] Y. Huang, Mol.Ther. Nucleic Acids 6 (2017) 116–132.
[12] B. Hu, L. Zhong, Y. Weng, et al., Signal Transduct. Target. Ther. 5 (2020), doi: http://dx.doi.org/10.1038/s41392-020-0207-x.
[13] Y. Chen, B. Li, X. Chen, et al., Chin. Chem. Lett. 31 (2020) 1153–1158.
[14] H. Gao, H. Feng, Y. Bai, et al., J. Biomed. Nanotechnol. 15 (2019) 1764–1770.
[15] M. Kim, G. Kim, D.W. Hwang, et al., J. Biomed. Nanotechnol. 15 (2019) 2401–2412.
[16] Y. Wang, F. Gao, X. Jiang, et al., J. Biomed. Nanotechnol. 15 (2019) 966–978.
[17] Z.L. Yu, J.X. Ye, X. Pei, et al., Acta Pharm. Sin. B 8 (2018) 116–126.
[18] S. Guo, Y. Huang, Q. Jiang, et al., ACS Nano 4 (2010) 5505–5511.
[19] X. Liu, M. Liu, J. Chen, et al., Chin. Chem. Lett. 29 (2018) 1321–1332.
[20] J.H. Lee, K. Lee, S.H. Moon, et al., Angew. Chem. Int. Ed. 48 (2009) 4174–4179.
[21] B.L. Liu, H.C. Zhang, Y. Ding, Chin. Chem. Lett. 29 (2018) 1725–1730.
[22] E.G. Liu, M. Zhang, H. Cui, et al., Acta Pharm. Sin. B 8 (2018) 956–968.
[23] J.F. Qu, T.H. Che, L.B. Shi, et al., Chin. Chem. Lett. 30 (2019) 1198–1203.
[24] Z. Abbasi, S. Rezayati, M. Bagheri, et al., Chin. Chem. Lett. 28 (2017) 75–82.
[25] F. Meng, J. Wang, Q. Ping, et al., Nano Lett. 19 (2019) 1479–1487.
[26] M.S. Mohamed, S. Veeranarayanan, T. Maekawa, D.S. Kumar, Adv. Drug Deliv. Rev. 138 (2019) 18–40.
[27] R. Mohammadpour, M.A. Dobrovolskaia, D.L. Cheney, et al., Adv. Drug Deliv. Rev. 144 (2019) 112–132.
[28] B. Liu, H. Zhang, Y. Ding, Chin. Chem. Lett. 29 (2018) 1725–1730.
[29] L. Yu, R. Han, X. Sang, et al., ACS Nano 12 (2018) 9051–9059.
[30] Y.K. Peng, Y.J. Tseng, C.L. Liu, et al., Nanoscale 7 (2015) 2676–2687.
[31] Y. Piao, J. Kim, H.B. Na, et al., Nat. Mater. 7 (2008) 242–247.
[32] W. Zhou, L. Guo, Chem. Soc. Rev. 44 (2015) 6697–6707.
[33] Y. Cui, X. Li, K. Zeljic, et al., ACS Appl. Mater. Interfaces 11 (2019) 38190–38204.
[34] Z. Wei, S. Luo, R. Xiao, et al., J. Hazard. Mater. 338 (2017) 472–481.
[35] L.F.O. Maia, R.C. Hott, P.C.C. Ladeira, et al., Chemosphere 215 (2019) 422–431.
[36] S.G. Chung, J.C. Ryu, M.K. Song, et al., J. Hazard. Mater. 267 (2014) 161–168.
[37] J. Wang, X. Li, Q. Cheng, et al., Carbohydr. Polym. 229 (2020) 115470.
[38] M. Xu, Y. Chen, G.B. Mao, et al., Mater. Express 9 (2019) 133–140.
[39] X. Li, W. Chen, L. Ma, et al., Chemosphere 195 (2018) 336–343.
[40] Y.K. Li, D. Li, K. Jian, et al., J. Biomed. Nanotechnol. 15 (2019) 85–99.
[41] C. Nayek, M.A. Al-Akhras, V. Narayanaswamy, et al., Mater. Express 9 (2019) 123–132.
[42] M. Chen, B. Tang, D.E. Nikles, IEEE. T. Magn. 34 (1998) 1141–1143.
[43] W.X. Chen, L.G. Yang, L.Y. Xu, et al., Biosci. Rep. 39 (2019) BSR20182062.
[44] S. Zheng, X. Wang, Y.H. Weng, et al., Mol. Ther. Nucleic Acids 12 (2018) 805–816.